The Effect of Monomolecular Films on the Rate of Gas Absorption into a Quiescent Liquid

R. E. PLEVAN and J. A. QUINN

University of Illinois, Urbana, Illinois

An experimental technique has been developed for measuring the permeability (or surface resistance) of various monolayers to gases, as well as their effectiveness in hindering any substrate motion which accompanies the absorption process. Results are reported for sulfur dioxide absorbing into water and into aqueous gels in the presence of several surface-active agents. Measured surface resistances extend from a maximum of 200 sec./cm. for a condensed layer of hexadecanol to an indeterminably small value for expanded and gaseous films. After an initial period in which transfer is by diffusion alone, convective motion sets in. The onset and magnitude of the convective motion is displayed by measured absorption rates into water covered with monomolecular films and into viscous gels. The relative magnitude of the convective retardation of the various films parallels their permeabilities, both effects being proportional to the compressibility of the monolayer.

That monomolecular layers of certain insoluble surface-active materials can drastically reduce the rate of transport of a gas through the gas-liquid interface is an established experimental observation; that this reduction in rate may be brought about directly by an interaction between the permeating gas molecules and the adsorbed layer or, indirectly, by suppressing convective motion within the fluid substrate is also widely recognized. What is not known is a detailed molecular explanation for the specific resistance of the monolayer in terms of measurable monolayer properties; nor is the coupling of substrate motion with the rheological behavior of the interface fully understood. In this paper we report experimental results in which the two aspects of the problem—the physicochemical and the hydrodynamic—have been separated; these results clearly show the relative effectiveness of various monolayers in hindering substrate motion.

The problem considered here is the permeation of a gas through a monolayer and into a liquid substrate in which the gas dissolves. A closely related problem is the evaporation of a pure liquid through a monolayer spread at the liquid-vapor surface. The latter problem has received considerable attention (*18, 19*) because of its practical application to water conservation. By comparison to the evaporation work, there have been relatively few studies of gas absorption in the presence of surface-active materials. [Literature in this area has been summarized by Davies and Rideal *(12).*] Of particular significance is the work of Blank (*4* to *8*); he has published experimental results on the transport of several gases through a series of different monolayers and he has also examined in considerable detail various theories of monolayer permeation. In addition, it should be noted that certain aspects of the present problem are closely related to the process of transport through natural membranes (*11*).

The present experiments were designed to eliminate some of the complicating factors which have obscured the interpretation of most previous work in this area. The experiment consisted of measuring the simultaneous response of two identical liquid layers—one covered by a monomolecular film of an insoluble surface-active material—to a step function in pressure of the absorbing gas. Measurements at small times, of the order of a few seconds, yielded values for the specific resistance of the monolayer, while long-time measurements showed the effect of the film on the convective rate of absorption. The validity of the technique was demonstrated by using the apparatus to measure the diffusivity of carbon dioxide in water. Further, to establish a scale for comparing the absorption rates with natural convection, the rate of absorption into aqueous gel solutions was also investigated.

EXPERIMENT

The Absorption Apparatus

A detailed section of one of the absorption cells is shown in Figure 1. A precision bore glass cylinder, 2.000 ± 0.0015 in. I.D. and 2 in. high, was held in compression between two stainless steel plates. Each plate contained a circular groove fitted with a rubber gasket to seal the glass. Soldered into each lower plate were two 16-gauge hypodermic needles, one extending 1⅝ in. upward into the cell and the other flush with the surface. Liquid was added to the cell through the flush needle, while surface-active agent was admitted through the longer needle. Capillary tubing (0.062 in. I.D.) was glued over the protruding lower ends of the needles so that the lines could be sealed with clamps.

The extension of the upper plate formed the barrel which housed the plunger. The inner bore of the barrel had been carefully machined and honed. The seal between the plunger and the barrel was made with a ⅛ in. thick Neoprene O ring, held in compression in a groove between the lower surface of the plunger and a removable disk.

The plunger of each cell was bolted to a common sliding assembly, mounted on three vertical support rods. The assembly was attached to the shaft of an air cylinder, a pneumatic device capable of producing a powerful linear stroke. Power to

the cylinder was supplied by compressed air and was controlled by a solenoid valve.

The free volume space above each absorbing liquid was connected to the tubing from the pressure transducer (bidirectional strain gauge, ± 0.3 lb./sq.in. range, Model 283 TC, Statham Instruments, Inc.) through an adapter mounted into the upper plate. A schematic of the pressure measurement system is shown in Figure 2.

Valve No. 1 isolated the two cells. When open, the pressure in each cell was equal; when closed, the pressure difference could be monitored by the transducer. The valve served as an emergency means of equalizing the pressures if the difference ever exceeded the safe operating range of the transducer. The No. 2 valves connected the system to the surroundings. Valves No. 3, 4, and 5 were required to protect the transducer from the corrosive sulfur dioxide gas. When a run was in progress, the No. 3 valves were open and No. 4 and 5 were shut. At all other times, however, the No. 3 valves were closed, thus isolating the large volume of sulfur dioxide in the absorption cells from a small amount of air which filled the transducer and its nearby connecting lines. With valves No. 4 and 5 open a slow purge of air was continually maintained. When carbon dioxide was the absorbing gas, these precautions were not necessary and the carbon dioxide filled the entire system.

The absorption apparatus rested in a large water bath. All portions of the absorption unit were submerged except for the transducer and a small segment of connecting tubing. The bath temperature was controlled at 24.5 ± 0.01°C., while room temperature was regulated at 24 ± 0.5°C.

Procedure

Prior to assembly the component parts of the absorption cell were thoroughly cleaned by soaking the glass sections in a hot chromic acid bath and flushing the stainless steel lower plates consecutively with water, ethyl ether, and acetone. After assembly, the system was tested for leaks by lowering the plungers to compress the gas and observing the pressure signal from the transducer. A constant signal indicated the absence of leaks, the probability that both sides would leak gas at exactly the same rate being small. A further check was made visually when water was in the bath.

With no leaks present the system was evacuated to remove air and the absorbing gas was bled in. Fifteen cubic centimeters of water, saturated with the absorbing gas, were added to the cells. For the runs in which the absolute rate of transfer was measured, liquid was added to only one cell; water was added to both cells for the difference measurements. To insure complete removal of any remaining inerts, gas was flushed through the system for 2 hr. The system was then allowed to equilibrate at the regulated temperature for at least 1 hr.

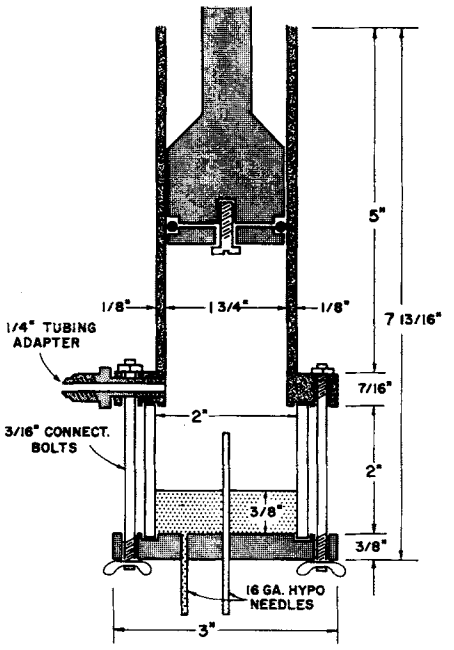

Fig. 1. The absorption cell.

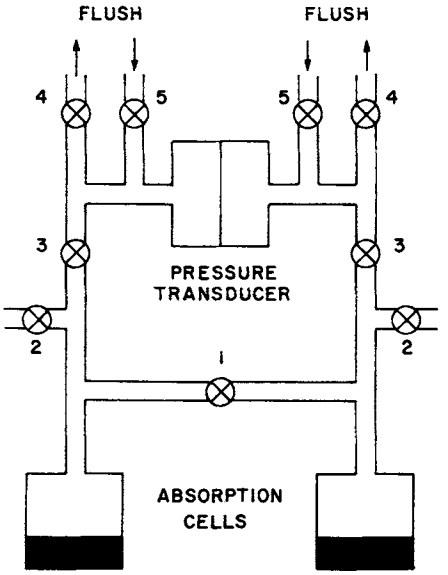

Fig. 2. Schematic drawing of pressure measurement system.

For the one-cell experiments a run was performed by lowering the plungers to compress the gas with the No. 1 valve open. When the plungers completed their stroke, the valve was closed to monitor the signal. Since one cell contained no liquid, the gas pressure on that side remained constant, and the transducer thus sensed only the decreasing pressure in the other cell.

Prior to adding the surface-active agent in the two-cell experiments, it was necessary to perform a blank run to verify that absorption was proceeding equally in both cells. The gas was compressed with the No. 1 valve closed, so that the pressure difference signal could be continuously monitored. A constant null signal confirmed the identical behavior of the absorption in each cell. Next 40 μliters of pure ethyl ether were added to the surface of one cell and gas was flushed through to remove the evaporating vapors. A check run was then performed to demonstrate that the spreading solvent had no effect on the absorption rate.

Forty microliters of the solution containing the surface-active agent were added to the surface of one cell by injecting it upward through the middle needle, forcing the solution out over the side. The solution trickled down the needle and exploded as it hit the surface, spreading the agent with it. If ethyl ether were used as the spreading solvent (see following section), the evaporating vapors were purged from the system by flushing with gas. Absorption runs with a monolayer on the liquid surface of one cell were performed identically to the blank runs.

Surface-Active Agents

The source and grade of the surface-active agents employed in this experiment are given in Table 1, together with their equilibrium spreading pressures (E.S.P.) on an acidic substrate (pH = 1.0). These surface pressures were measured independently in a Langmuir trough on an aqueous sulfuric acid solution substrate which closely approximated the 0.8 pH of the saturated sulfur dioxide–water medium used in the actual experiment.

The oleic acid and dodecyltrimethyl ammonium chloride (50% solution in an unknown solvent) were liquids. Each was spread onto the liquid surface directly without need of an additional solvent. The remaining five agents were solids. Cholesterol was spread from a saturated solution in ethyl ether, while the other four were spread from a 1% by weight solution in ethyl ether. All agents were added in substantial excess of the amount required to form just one layer. The excess material for the solid agents adhered to the walls of the cell, while for the liquid agents it remained as a small lens on the surface. Comparable excesses were used in measuring the equilibrium

TABLE 1. PROPERTIES OF SURFACE-ACTIVE AGENTS

Agent	Grade	Source	Surface state ($pH = 0.8$)	E.S.P. (dynes/cm.) on sulfuric acid-water substrate ($pH = 1.0$)
1-Hexadecanol	Practical	Matheson, Coleman, and Bell	Condensed	46
1-Octadecanol	—	Eastman Organic Chemicals	Condensed	40
Stearic acid	U.S.P.	Fisher Scientific Co.	Condensed	20
Oleic acid	U.S.P.	J. T. Baker Chemical Co.	Expanded	31
Cholesterol	U.S.P.	Nutritional Biochemicals Corp.	Condensed	35
Hexadecylamine	Technical	Eastman Organic Chemicals	Gaseous	33
Dodecyltrimethyl ammonium chloride	—	K. and K. Laboratories, Inc.	Gaseous	31

spreading pressures in the trough experiments. Apparently, this excess material did not alter the overall resistance of the film by any measurable amount (22).

ANALYSIS OF THE PRESSURE RESPONSE

Two types of experiments were performed. First, absolute rates of absorption were measured to determine diffusion coefficients in the absorbing medium. Second, the net rate of absorption between two identical cells, one of which contained surface-active material, was measured in order to obtain information on specific surface resistances. In both cases the variable recorded was the decay in time of the pressure of the absorbing gas following an initial step function in gas pressure. In this section we describe the mathematical analysis whereby the diffusion coefficients and surface resistances were calculated from the measured pressure response.

Diffusion Calculations

The free space above the liquid in the absorption cell contained pure gas saturated with water vapor. As absorption proceeded the number of moles in the constant volume gas space diminished; thus

$$n(t) = n_o - A\int_o^t N\,dt \tag{1}$$

Equation (1) is actually a relation between the concentration and mass flux at the gas-liquid surface. This may be seen more readily by taking the time derivative and substituting (1) for the number of moles in terms of the volume, temperature, and pressure of the gas and (2) introducing Henry's law in the form

$$\frac{c_i}{P_i} = \frac{c_o}{P_o} = \frac{c_s(t)}{P(t)} = H \tag{2}$$

where H is a function of temperature alone. The rearranged form of Equation (1) is then

$$\frac{dc_s}{dt} = \left[\frac{AHRT}{V}\right] D\frac{\partial c}{\partial x}(0,t) \tag{3}$$

Diffusion within the liquid substrate (presumed semi-infinite) is governed by

$$\frac{\partial c}{\partial t} = D\frac{\partial^2 c}{\partial x^2} \tag{4}$$

with the initial and boundary conditions

$$c(x,0) = c(\infty,t) = c_i \tag{5}$$

By comparison to the analogous heat conduction problem (9), the solution of Equations (3), (4), and (5) gives the surface concentration $[c_s(t) = c(0,t)]$ as

$$\frac{c_o - c_s}{c_o - c_i} = \frac{P_o - P(t)}{P_o - P_i} = 1 - \exp[y^2]\,\mathrm{erfc}[y] \tag{6}$$

where

$$y = k\sqrt{t}, \qquad k = \frac{AHRT}{V}\sqrt{D} \tag{7}$$

The correct pressure terms to be substituted into the left side of Equation (6) are the partial pressures of the absorbing gas at the appropriate conditions. Since the absorbing gas in the free volume space is always saturated with water vapor, the gas partial pressure is equal to the total pressure in the cell minus the vapor pressure of water. But since the vapor pressure appears in all four terms it subtracts out, and thus Equation (6) becomes a valid relationship for the total pressure in the cell, the variable actually measured with the transducer.

A more convenient form for Equation (6) is obtained by expanding the right-hand side in a power series:

$$\frac{P_o - P(t)}{P_o - P_i} = \frac{2}{\sqrt{\Pi}}y - y^2 + \frac{4}{3\sqrt{\Pi}}y^3 - \dots \tag{8}$$

It should be noted here that the first term in the expansion is the exact solution for the pressure response for the case of absorption with a constant surface concentration.

Since the first term of Equation (8) was the dominant term in all present measurements, the following method of calculation was adopted. The relative pressure change was plotted as a function of the square root of time. By selecting two points from these data, the quotient

$$S = \frac{\left[\dfrac{P_1 - P_2}{P_o - P_i}\right]}{\sqrt{t_2} - \sqrt{t_1}} \tag{9}$$

was formed. Obviously, for small values of time the curve will be approximately linear, with a constant slope equal to S. Substitution for P_1 and P_2 from Equation (8) yields S as a function of y_1 and y_2. Further, if in substituting Equation (8) all terms higher than the second are discarded, then the resulting equation will be quadratic in k. This final equation in k may be expanded to the computational form

$$k = \frac{\sqrt{\Pi}}{2}S\left\{1 + \frac{1}{4}(\Pi\,\alpha\,S) + \frac{1}{8}(\Pi\,\alpha\,S)^2 + \dots\right\}$$

where

$$\alpha = (\sqrt{t_1} + \sqrt{t_2}) \tag{10}$$

The diffusion coefficients discussed below were calculated by using Equation (10).

Surface Resistance

For absorption into a stagnant liquid layer, the diffusional resistance of the liquid increases with the square root of contact time, attaining a value of about 500 sec./

cm. at the end of 1 sec. (12). Relative to such bulk phase resistances, the resistance of most monolayers is small, with the result that the monolayer has an appreciable effect on the absorption rate only at very short contact times. As an example, with a typical value of surface resistance of 100 sec./cm., the overall rate is reduced by less than 20% at the end of 1 sec. In the present experiments the effect of the monolayer was accentuated by measuring the difference in integrated rate, that is, total amount absorbed, between two separate absorption cells, one of which contained surface-active material.

In the analysis below we presume that at small times changes in the gas pressure, and hence changes in the gas phase composition immediately adjacent to the surface layer, are determined solely by changes in the volume of the gas space. This is, of course, an idealization inasmuch as the pressure changes both because the volume of the gas space is changing and because gas is being absorbed. However, for short times—and in examining surface resistances we are interested only in events which occur within the first few seconds—we may safely neglect the latter effect. This treatment is equivalent to assuming that for small t the pressure response is given by the first term of Equation (8).

Ideally, the absorbing gas undergoes a step increase in pressure at $t = 0$. Experimentally, the change in gas pressure occurs over some finite time interval. Here it is assumed that the gas is pressurized in some arbitrary manner described by $F(t)$. In the cell containing pure liquid the surface boundary condition is identical to Equation (2), here written as

$$c_1(0, t) = H F(t) \tag{11}$$

For the cell in which the liquid surface is covered with a monolayer, we use the following model to describe the flux through the layer:

$$-D\frac{\partial c_2}{\partial x}(0, t) = k_s [H F(t) - c_2(0, t)] \tag{12}$$

where k_s, the mass transfer coefficient through the surface layer, is a measure of the permeability of the monolayer. Solution of Equation (4) with Equation (5) and either (11) or (12) gives the absorption rate for the two cases. The result needed here, however, can be obtained without a complete solution of the equations.

The pressure response is proportional to the integrated absorption rate:

$$Q = \int_o^t \left[-D\frac{\partial c}{\partial x}(0, t) \right] dt \tag{13}$$

Note that in the limit

$$\lim_{t\to\infty} Q = \int_o^\infty \left[-D\frac{\partial c}{\partial x}(0, t) \right] dt = -D \lim_{s\to 0} \frac{d\bar{c}}{dx}(0, s) \tag{14}$$

where $\bar{c}(x, s)$ is the Laplace transform of $c(x, t)$. The limiting value for the difference in total absorption rate for the two cases is, therefore

$$\lim_{t\to\infty} [Q_1 - Q_2] = -D \lim_{s\to 0} \left[\frac{d\bar{c}_1}{dx}(0, s) - \frac{d\bar{c}_2}{dx}(0, s) \right] \tag{15}$$

The derivative terms can be evaluated from the transformed boundary conditions and Equation (4). As s approaches zero the limit is obtained by use of the final-value theorem (23) with the result that

$$\lim_{t\to\infty} [Q_1 - Q_2] = \frac{D}{k_s} [H F(\infty) - c_i] \tag{16}$$

$F(\infty)$ represents the pressure at the end of the step change and $H F(\infty)$ is the equilibrium concentration corresponding to this pressure. The primary importance of this result is that it demonstrates that the determination of k_s is independent of the particular manner in which the change in pressure is brought about. As long as the change occurs identically in both cells, only the final value of pressure is required.

Since the complete retarding effect of the monolayer is manifest after the first few seconds of absorption, the limiting value of time indicated in Equation (16) is attained, practically, 10 to 20 sec. after the pressure change. The application of the analysis is discussed below.

RESULTS AND DISCUSSION

Diffusion Studies

In measuring diffusion coefficients, absorbing solution was placed in one of the two cells, leaving the other empty so that absolute rates could be determined. Typical results for carbon dioxide are shown in Figure 3 where the amount absorbed Q is shown as a function of the square root of time. Q is proportional to the change in absorbing gas pressure, which, for small values of time, varies with $\sqrt{t}$ as shown by Equation (8).

In these runs, the first data were obtained after an exposure of 24 sec. Prior to this time an anomalous temperature effect (further discussed below), occurring unequally in each cell, was superimposed on the pressure curve. The appropriate P_o was therefore obtained by extrapolating linearly the curve of P vs. $\sqrt{t}$ to zero time. The moles of gas transferred were then calculated from the pressure data. The results shown in Figure 3 represent the average of from four to six replicate experiments with the reproducibility between runs better than 5%. Although discrete points are depicted in this and subsequent figures, it should be noted that the pressure response was recorded as a continuous curve; points at selected time intervals were chosen for representation.

For absorption into water, the rate data begin to diverge from the predicted curve after approximately 90 sec. Beyond this time the measured rate increases markedly with the result that the amount of gas absorbed at $t = 5$ min. is twice that which would be calculated for pure diffusional transport. The divergence of the measured and calculated rates marks the onset of convective motion within the substrate. Since a solution of carbon dioxide in water is more dense than pure water, the ab-

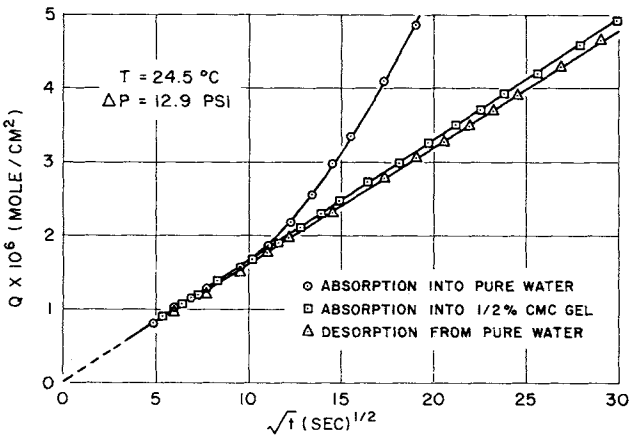

Fig. 3. Transfer of carbon dioxide into aqueous solutions.

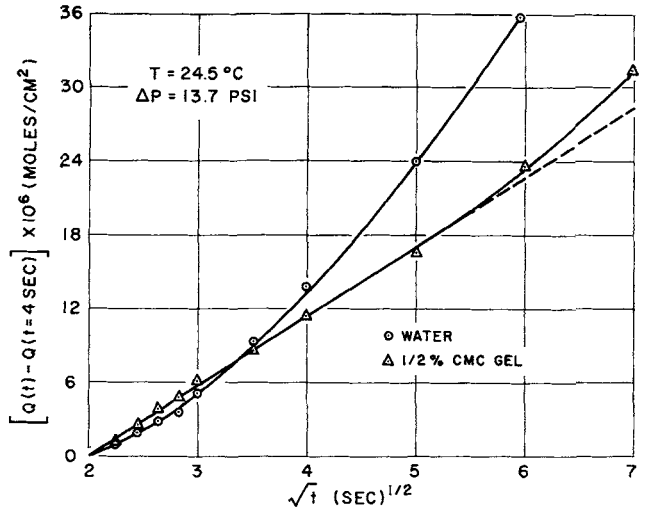

Fig. 4. Transfer of sulfur dioxide into aqueous solutions.

sorbing solution is potentially unstable with respect to buoyancy forces. If indeed the convection is buoyancy-driven then a saturated fluid layer should be stable when undergoing desorption. That convection is absent for the desorption can readily be seen in Figure 3 where desorption data, for a step change in pressure exactly the same as the absorption runs, are shown for a 15-min. interval. Over the entire time range the data agree remarkably well with predicted behavior. Further, whatever the mechanism of the convection, with a more viscous fluid the onset of the motion should be delayed and the intensity of the convective currents should diminish. This is confirmed by the results on absorption into a 0.5% CMC gel. The apparent viscosity of the gel (50 centipoise) was sufficient to prevent motion, and as shown in Figure 3 absorption into the gel agreed closely with the desorption data.

By using Equation (10), diffusion coefficients can be calculated from the pressure response. The solubility of carbon dioxide in water at 25°C. and under a partial pressure of 760 mm. was taken as 3.39×10^{-5} g.-moles/cc. (*14*). Values obtained from the desorption runs and from the initial portion of the absorption runs are within 3% of the accepted value, namely, 1.97×10^{-5} sq. cm./sec. at 25°C. (*24*). This agreement substantiates assumptions made in the analysis and it also demonstrates the precision inherent in the experimental technique.

In Figure 4 comparable data are shown for the absorption of sulfur dioxide into water and into a 0.5% CMC gel. The time $t = 4$ sec. was selected as the reference point for comparing the data, the absorption rate having been measured from that time. (The 4-sec. time delay was due to the closing of the No. 1 valve, as previously explained.) Also, since the absolute rate of absorption with sulfur dioxide was considerably larger than with carbon dioxide, the anomalous temperature effect did not distort these data.

Since sulfur dioxide is approximately seventy-five times more soluble in water than carbon dioxide, and since saturated solutions of the former are considerably more dense than the latter, it is to be expected that convection will set in at a smaller time and with greater intensity for sulfur dioxide as compared with carbon dioxide. Figure 4 indicates that with pure water measurable convection commenced at about 7 sec.—as opposed to 90 sec. with carbon dioxide—and in the gel at 35 sec., whereas no convection had been observed in the gel with carbon dioxide for times as long as 15 min. At short times the water data of Figure 4 fall slightly above those for the gel. This small difference is of the order of the experimental accuracy at these times and for this reason it is not considered significant. Unfortunately, it was not possible to perform desorption runs with sulfur dioxide, because on lowering the pressure over a saturated solution, numerous bubbles of the highly soluble gas were nucleated at the bottom of the cell.

Diffusion coefficients calculated for sulfur dioxide were lower than the accepted value (*20*) (see below). As an example, 1.2×10^{-5} sq. cm./sec. was the value calculated for the 0.5% CMC gel. For pure water, the time interval over which meaningful diffusion data were obtained, 4 to 7 sec., was not well enough defined to permit accurate calculations. All results were, however, of the proper order of magnitude, and they were considered to be sufficiently accurate to justify the analysis. Also, in all calculations it is assumed that the temperature of the interface is constant even though the gas temperature changes on compression (see discussion in following section) and the liquid near the interface is heated by the small heat of solution. A thermocouple placed in the liquid approximately 0.05 cm. from the interface registered a maximum temperature rise of 0.1°C.

Experiments with Monomolecular Films

In the net absorption runs, various surface-active agents were deposited (at their equilibrium spreading pressures) on the absorbing solution in one of the cells with the other cell containing pure solution. Results for sulfur dioxide permeating through a film of hexadecanol (cetyl alcohol) are shown in Figure 5. The dashed section of the curves represents the measured response at small times with a slight imbalance in gas temperature in the two cells. The solid lines show the true pressure response due to the absorption process.

The initial step change in pressure in the two cells was brought about by halving the gas volume of both cells. This change in pressure corresponds to a calculated adiabatic temperature rise of the gas of approximately 100°C. However, because of the small heat capacity and large surface area of the gas space, this temperature increase rapidly diminished, with the gas cooling to ambient temperature within the first few seconds of the experiment. A thermocouple placed in the gas space indicated an actual temperature increase of only 20°C. with the temperature of both cells dropping to within 2° of the bath temperature in the first 10 sec. No temperature difference could be detected after 20 sec. Thermocouple measurements further showed that the temperature rise in one

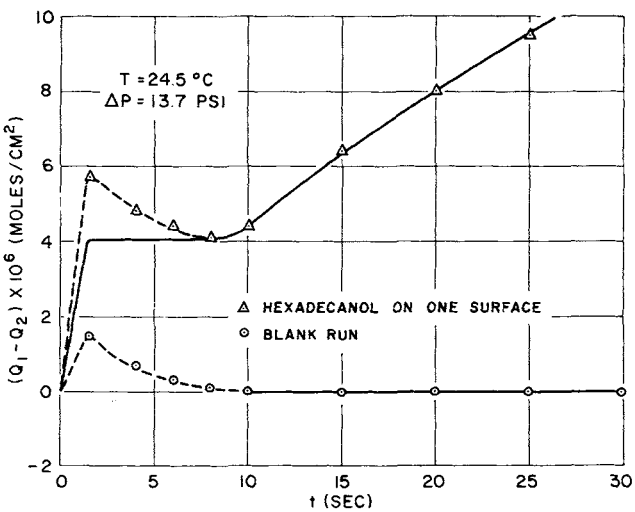

Fig. 5. Effect of hexadecanol on sulfur dioxide absorption into water.

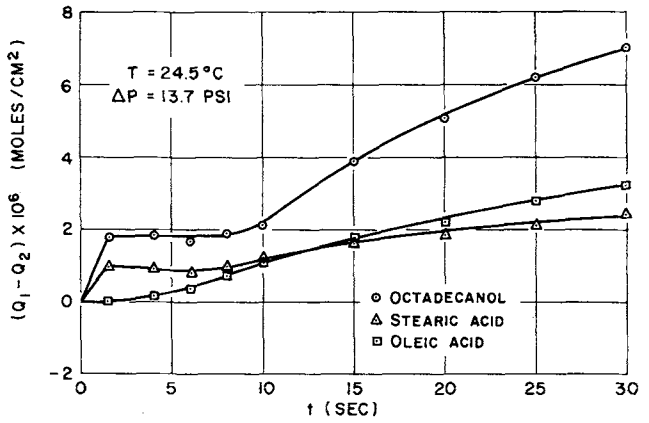

Fig. 6. Effect of monolayers on sulfur dioxide absorption into water.

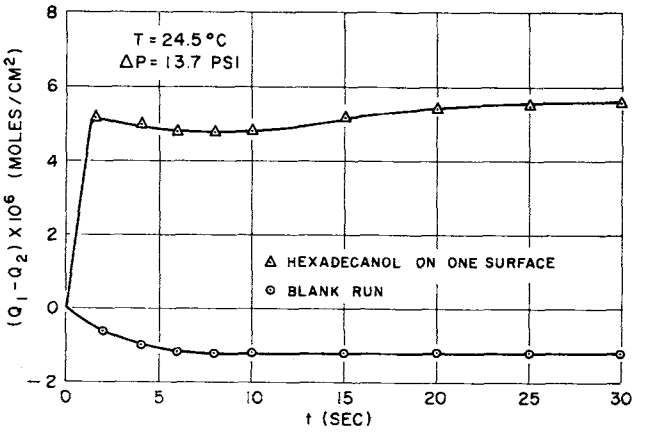

Fig. 7. Effect of hexadecanol on sulfur dioxide absorption into 0.5% CMC gel.

cell was consistently 2°C. higher than in the other cell. This troublesome difference in temperature was most likely caused by unequal frictional heating of the gas in the two cells, brought about by imperfect alignment of the cylinders or a tighter compression of the O ring in one cell. This slight imbalance in temperature resulted in the spurious pressure rise shown by the dashed line in Figure 5. In subsequent discussion this temperature effect has been eliminated by subtracting the initial temperature peak (as given by a blank run) from the absorption response curves of the monolayer experiments.

The first requirement in performing a net absorption run was to demonstrate that with pure solution in both cells the response, and therefore absorption rate, was identical in both cells. Under proper conditions, the blank run gave a null signal such as the horizontal line through the origin shown in Figure 5. With a monolayer spread on one solution, the characteristic pressure response exhibited two distinct regions. The first region extended to $t = 7$ sec. with the pressure change almost stepwise. (The initial linear change from zero pressure coincided with the piston movement.) Beyond $t = 7$ sec. the pressure difference, or net total absorption as shown in Figure 5, increased linearly to the termination of the run.

The initial displacement of the curve is the result of the surface resistance of the monolayer, the magnitude of which can be calculated by using Equation (16). This effect is evident well before any fluid motion in the substrate commences and is, therefore, solely a result of the physicochemical properties of the monolayer. The second portion of the curve displays the effect of convection, with the steadily increasing difference in amounts absorbed in the two cells indicating that the monolayer is effective in suppressing motion, thereby lowering the absorption rate. Additional verification on these points was obtained by schlieren photography of the substrate (discussed below).

Results with three different surface-active materials are shown in Figure 6. Each of the curves has the same general behavior as that of hexadecanol, with oleic acid showing negligible surface resistance. Net absorption into a gel is typified by the data of Figure 7 for hexadecanol spread on a ½% CMC gel. Here convective motion is absent over the first 30 sec. and the anticipated step change is observed. [The blank run of Figure 7 is displaced from the zero line as a consequence of a slight difference (less than 0.3 cc.) in free volume in the two cells. Even though slightly unbalanced, a surface resistance can be calculated from the displacement of the two curves.]

Pertinent information obtained from the experiments with various monolayers is summarized in Table 2. Values of the surface resistance have been calculated from Equation (16) with a Henry's law constant of 1.52×10^{-3} g.-moles/(cc.)(atm.) at 25°C. used throughout (*14*). The numerical value of the diffusion coefficient used in the computations was 1.46×10^{-5} sq. cm./sec. at 20°C. (*20*), corrected for temperature with the Nernst-Einstein relationship. Each entry in the table represents the average of at least two replicate runs with a given monolayer. Note that one important advantage of the present technique over most previous studies of this type is that once balanced and sealed, successive absorption runs can be run indefinitely with a fixed monolayer and substrate. In several instances, replicate runs extended over a period of days with excellent agreement between runs. Typically, the reproducibility between runs was approximately 5% with a maximum deviation of 10%. Two separate entries for octadecanol and four for hexadecanol (at 24.5°C.) show the agreement between different series of experiments, each series performed with a fresh substrate and monolayer. The spread in values, 20 to 30%, is indicative of the precision with which the surface resistances could be measured. For some of the monolayers, no surface resistance was detected and for these materials $R_s = 0$ is listed in Table 2. Obviously, this does not mean that the resistance is truly zero; rather, none could be detected by the present technique.

As a measure of the effectiveness of a monolayer in suppressing convective motion, several different param-

Table 2. Surface Resistance and Convective Retardation of Monolayers*

Agent	R_s, sec./cm.	$\left(\frac{Q_1 - Q_2}{A}\right)/t \times 10^7$, moles/(sq. cm.)(sec.)
Hexadecanol	215	—
	165	3.3
	170	3.4
Octadecanol	85	2.4
	80	2.1
Stearic acid	35	0.7
Oleic acid	0	1.2
Cholesterol	0	1.1
Dodecyltrimethyl ammonium chloride	0	0.3
Hexadecylamine	0	0.3
Hexadecanol		
$T = 14.5$°C.	235	3.8
$T = 24.5$°C.	175	2.9
$T = 32.4$°C.	120	2.3
Hexadecanol on 0.5% CMC gel	250	0.5

* At 24.5°C., unless otherwise noted.

eters could be calculated from the net absorption data. The one arbitrarily chosen here and listed in the second column of Table 2 was the average slope of the absorption difference curve between $t = 10$ and 30 sec.

In interpreting the convective rates in the presence of a monolayer, it should be noted that in the two cell experiments, the difference in absorption rates may not be entirely due to the fact that the monolayer suppresses convective motion. If any convective motion occurs in the fluid phase beneath the monolayer, then the effective resistance of the bulk phase will be smaller than that of a stagnant layer. For this reason the ratio of monolayer to bulk phase resistance will be greater with substrate motion and, therefore, the relative effect of the monolayer will be manifest over a longer time than in the case of a truly stagnant liquid.

Note also that the net convective rates presented here are conservative. That is, at any given instant the pressure, and hence the equilibrium surface concentration, is greater in the cell containing the monolayer, since a smaller amount of gas has been absorbed from the closed gas space. Thus the smaller permeability through the monolayer is partially offset by a larger concentration difference across the layer. If one were to keep the gas pressure the same in both cells throughout a run, the net absorption rates would be larger than those reported here.

Monolayer Properties

Before attempting to explain these results it is necessary to cite particular properties of the films which influence their surface behavior. Monolayers are classified as condensed, expanded, or gaseous, depending on the extent of the cohesive forces between the molecules; these forces are reflected in the surface pressure area isotherms (*1*). One of the factors which exerts a pronounced effect on the state of the monolayer is the *p*H of the substrate. Long-chain fatty acids, for example, ionize to form gaseous films on strongly alkaline substrates (*p*H $\geq$ 12), but otherwise form condensed films. Amines exhibit opposite behavior; they ionize on acidic solutions but remain condensed on neutral and alkaline substrates. The greatest stability is shown by the alcohols, which exist in the condensed state over almost the entire *p*H range.

The *p*H of the sulfur dioxide-water substrate in the present experiments was 0.8. This value was calculated from the first ionization constant of sulfurous acid (*22*) and was verified with a *p*H indicator. The state of each of the monolayers used in this work is listed in Table 1 for a *p*H of 0.8 (*12, 17*).

By virtue of the method of depositing the surface-active agent, the surface pressure of each film was fixed at a unique value—the equilibrium spreading pressure. Here, surface pressures were not measured in the absorption cell, but independently on a Langmuir-Adam film balance equipped with a Cenco du Nuoy torsion head for measuring film pressures (*22*). Agents were spread on a sulfuric acid solution (*p*H = 1) which approximated experimental conditions and on pure water for comparison. Results are shown in Table 1 along with literature values.

The relative surface pressures and concentrations can best be seen on a pressure area diagram such as Figure 8. The isotherms plotted on Figure 8 have been taken from the literature and are believed to be representative of the materials and conditions used in the present work. The solid points designate the equilibrium spreading pressures which obtained in the absorption cell.

In dealing with the dynamic behavior of a monomolecular film, the two properties of interest are the surface viscosity and elasticity, with the latter property being more important in the present study. The elasticity, in turn, is related to the monolayer compressibility, defined as (*12*):

$$C_s = -\frac{1}{A}\left(\frac{\partial A}{\partial \Pi}\right)_T$$

with a range of values extending from infinity for a clean surface to, typically, 10^{-3} cm./dyne for a condensed layer. Note that C_s can be evaluated directly from a Π-A isotherm and that the slopes of the various curves in Figure 8 show the relative compressibilities at the equilibrium spreading pressures used here.

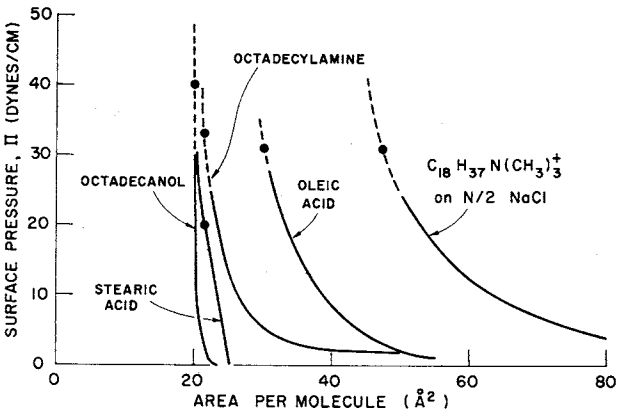

Fig. 8. Surface pressure area curves for monolayers.

Relative Effects of the Various Films

In this section the relative effects of the various films are examined along with qualitative explanations for some aspects of the data. No attempt is made to review the various theories of monolayer permeation (*8, 13*).

It can be seen from Table 2 that with some exceptions the magnitude of the surface resistance parallels the convective retardation of the film. This suggests that there may be some property of the monolayer which is involved in both phenomena. If, following Blank (*8*), we assume that the permeability of a monolayer depends on both the free area in the layer as well as fluctuations in monolayer density (which give instantaneous, local expansions increasing the free area), then the surface resistance should be proportional to the surface compressibility. The ability of the layer to resist shear and thereby retard substrate motion is also proportional to C_s. One would then expect the following order for both surface resistances and convective retardation: condensed > expanded > gaseous films. This is, of course, an oversimplification, since no mention has been made of the surface orientation of the adsorbed molecules, a factor which determines the free area in the layer.

The compressibility criterion is applicable only in comparing layers similar in structure. Thus with stearic acid and octadecanol, which are chemically identical except for the hydrophilic group, the ratio of compressibilities (about 5) is in rough agreement with the ratio of resistances and the ratio of retardation coefficients. This compressibility ratio comes about because the acid exerts a spreading pressure only one-half that of the alcohol and at the lower pressure the acid has a correspondingly higher compressibility (see Figure 8).

The results for octadecanol and hexadecanol are inconsistent with this explanation. The Π-A curves are essentially the same (*1*) and their spreading pressures are comparable. Nevertheless, both convective and resistive effects are substantially greater for the hexadecanol. Blank (*5*) has made a similar observation (on convection) and he concludes: "The only way in which the two films differ considerably is in their spreading rates, and if both films were disrupted because of heating or convection, then the

C_{16} alcohol would recover more quickly and show a greater effect."

Blank was unable to calculate surface resistances from his measurements on sulfur dioxide but, presumably, the greater spreading rate would lead to a higher surface resistance by the density fluctuation argument.

A lower spreading rate may also explain the results with oleic acid and cholesterol. Cholesterol, though least compressible of all the monolayers, retards convection only one-third to one-half as effectively as the alcohols. This may well be related to the expected lower spreading rate of this bulky molecule. On the other hand, oleic acid exerts a retardation effect much larger than would be indicated by its compressibility. Possibly the high value of C_s is offset by its greater spreading power. Oleic acid was the only agent introduced as a pure substance and any excess acid would remain as a lens on the surface. The lens acting as a reservoir to maintain a constant surface pressure and to replenish the film if disrupted. The absence of a surface resistance with both oleic acid and cholesterol is readily explained in terms of the relatively large free surface areas in these monolayers. Those agents which gave a surface resistance all formed close-packed monolayers, with surface areas of 20 to 22 Å.^{2}/molecule (Figure 8). The oleic acid, however, gave a surface area of approximately 30 Å.^{2}/molecule and cholesterol, with its multiple ring structure, formed a film which was more porous than the films of the straight chain compounds.

The last group of compounds formed gaseous films with high permeability and compressibility. Both the hexadecyl amine and the dodecyltrimethyl ammonium chloride showed little retardation and their behavior is consistent with the ordering in terms of compressibility.

Permeabilities Compared With Previous Work

The most comprehensive studies of monolayer permeabilities have been reported by Blank (*4, 5*). His values of k_s for carbon dioxide, oxygen, and nitrous oxide are of the same order of magnitude as present determinations for sulfur dioxide. Whitaker and Pigford (*27*), who used a frequency response technique, measured absorption rates of sulfur dioxide into water which contained cresol red as the surface-active indicator. Though interpreting their results in terms of a different surface model (involving three independent rate constants), it would appear that the value which they calculate for the resistance of cresol red is smaller than the minimum value which could be detected here (10 to 20 sec./cm.). Harvey and Smith (*15*) studied the transfer of carbon dioxide into pure water and into aqueous solutions of Lissapol and Teepol, commercial detergents. With an interferometric method they detected surface resistances comparable to our values for stearic acid.

Usual theories of monolayer permeation treat the transfer problem as an activated process with the permeating molecule encountering a potential energy barrier at the surface. With this in mind, we measured the surface resistance of the most effective agent, hexadecanol, at temperatures of 14.5°, 24.5°, and 32.4°C. The results are listed in Table 2. The least-squares line through the data gives an experimental activation energy of 6,550 cal./mole. This value is larger than Blank's (*5*) calculated energy for carbon dioxide permeation (2,000 cal./mole) but smaller than Barnes and La Mer's (*2*) value for evaporation resistance (approximately 10,300 cal./mole). Barnes and La Mer subdivide the activation energy into two parts: one part due to the hydrophilic group and the terminal methyl group of the molecules, and the other part due to the methylene groups of the straight chain. Curiously, the energy measured here is very close to the total value (6,460 cal./mole) ascribed to the terminal groups of hexadecanol from the evaporation study.

Convective Motion and Schlieren Photography

The convection currents observed in these experiments could be caused by: density gradients in the fluid layer, that is, natural or buoyancy-driven convection; surface tension gradients in the free surface, a so-called surface-tension-driven flow or interfacial turbulence (*3, 26*). The motion accompanying the absorption of carbon dioxide would appear to be buoyancy driven for the reasons given above, the principal one being the absence of convection with desorption. This conclusion is supported by Goodridge (*13*) in a recent article in which he states that the system carbon dioxide-water does not exhibit any interfacial turbulence.

To examine the convective motion, some additional experiments with surface-active agents were performed with carbon dioxide. Surprisingly, the added agent had no observable effect on the convection rate. (Surface resistance measurements could not be made with carbon dioxide because of its low solubility and, hence, small absolute absorption rate.) The fact that the agent had no effect suggests that the surface of the pure solution was contaminated prior to the spreading of the surface-active agent. If indeed the convection is buoyancy driven then the only way in which the surface conditions influence the motion is by way of the surface boundary condition, the extremes of which are that the surface is free or fixed. On the basis of linear stability analysis (*10*) the critical Rayleigh number (that dimensionless group which characterizes the motion) for the two cases differs by a factor of probably less than two. Calculated Rayleigh numbers (*22*), based on the depth of penetration, show that at the time convection was first observed, the Rayleigh number was at least an order of magnitude greater than the critical value predicted from linear theory. That the surface of the solution was most likely contaminated with some insoluble surface-active material is not surprising, since almost all stagnant liquid surfaces contain impurities (*16*).

In contrast, the sulfur dioxide experiments suggest surface-tension-driven flow coupled with the buoyancy mechanism. As discussed above the added films had a pronounced effect on convection accompanying the absorption of sulfur dioxide. Such large effects might be expected with surface-driven flows, since the elasticity and viscosity of the surface layer determine the magnitude of the convection. Curiously, convection did not appear immediately but after 7 sec. with water and after about 30 sec. with the ½% (50 centipoise) gel. This initial period may represent the time required for a disturbance to grow to a size large enough to be observed, though it is not obvious why times of this order would be required.

A possible explanation for the time delay is that the surface tension mechanism was triggered by buoyancy-driven flow. The sequence would be: as absorption commences, the concentration boundary layer grows (with the square root of time) until the fluid layer beneath the absorbing surface is unstable with respect to the density gradient. Motion ensues with shear forces being exerted on the stagnant layer. Under the shearing force the layer yields, giving alternate regions of low and high compression—regions of low and high permeability. With nonuniform absorption rate over the surface, gradients in surface concentration and temperature would re-enforce the local surface pressure gradients, thereby establishing all the necessary conditions for a sustained convective flow.

To examine further the convective circulation an optical apparatus was set up for viewing the absorbing solution with a schlieren light beam (*21, 25*). With this arrangement density gradients in the fluid could be viewed

through the side of a rectangular (to minimize optical distortion) prototype cell. Unfortunately, the meniscus at the wall of the cell obscured the region within a millimeter of the gas-liquid surface. Motion pictures of the circulation patterns with sulfur dioxide coincided exactly with the onset of motion as indicated by the measured absorption rate. The onset appeared as a two-dimensional wave breaking off and plunging down from the liquid surface. This pattern resembled a shock wave moving through the fluid. Following this front the motion set in as a series of narrow, vertical columns, with fluid raining through the columns. The patterns with a film spread on the surface and the motion in a gel were similar, though less vigorous, than those with water alone.

No density patterns were seen with carbon dioxide. The density differences, and also the refractive index differences, are at least 20 times smaller with carbon dioxide than with sulfur dioxide and the convective circulation is also much smaller. The fact that motion was not seen most likely indicates that the circulation was close to the surface (partly hidden by the meniscus at the wall) and that the density gradients were small. With more sensitive optical equipment, motion would probably be observed.

CONCLUSIONS

By the experimental technique reported here it is possible to separate the diffusive and convective effects accompanying gas absorption in the presence of monomolecular films. Close-packed monolayers of several surface-active materials have been shown to retard the absorption of sulfur dioxide into water by presenting a surface resistance as well as suppressing convective motion. Qualitatively, these effects can be correlated in terms of the physical properties of the monolayer, with the surface compressibility being of prime importance. Quantitatively, the magnitude of the measured surface resistances is comparable with related literature values.

With carbon dioxide absorbing into water, convection appears to be density driven; with sulfur dioxide, both surface forces and buoyancy forces are involved. The absorption data provide information on the onset and growth of convective circulation in water and in viscous gels, with and without an elastic surface layer. A possible explanation for the flow observed with sulfur dioxide is that the surface-driven mechanism is triggered by buoyancy forces.

ACKNOWLEDGMENT

This investigation was supported in part by the U. S. Public Health Service under Research Grant WP-00601. Fellowships received by R. E. Plevan from the National Science Foundation and from the American Oil Company are gratefully acknowledged. Preliminary experiments on the absorption apparatus were performed by E. Elzy and R. D. Hall.

NOTATION

A = area, sq. cm.
c = concentration, g.-moles/cc.
c_s = surface concentration, g.-moles/cc.
C_s = monolayer compressibility, cm./dyne
D = diffusivity, sq. cm./sec.
E_a = activation energy, cal./g.-mole
$F(t)$ = applied pressure defined by Equation (11), atm.
H = Henry's law constant, g.-moles/(cc.)(atm.)
k = constant defined by Equation (7), sec.$^{-1/2}$
k_s = surface mass transfer coefficient, cm./sec.
n = moles of gas, g.-moles
N = instantaneous absorption rate, g.-moles/(sq. cm.)(sec.)
P = instantaneous gas pressure, atm.
Q = total amount absorbed, defined by Equation (13), g.-moles/sq. cm.
R = gas constant, 82.05 (cc.)(atm.)/(g.-mole)(°K.)
R_s = surface resistance, equals $1/k_s$, sec./cm.
s = transform variable, defined following Equation (14)
S = slope of response data, defined by Equation (9), sec.$^{-1/2}$
T = absolute temperature, °K.
V = volume of gas space, cc.
x = distance normal to gas-liquid surface, cm.
y = dimensionless variable defined by Equation (7)

Greek Letters

α = variable defined following Equation (10), sec.$^{-1/2}$
Π = surface pressure, dynes/cm.

Subscripts

i = conditions at $t \leq 0$
0 = limiting conditions as $t \rightarrow 0+$
1 = absorption into a pure liquid
2 = absorption into a liquid covered with a monomolecular film

LITERATURE CITED

1. Adam, N. K., "The Physics and Chemistry of Surfaces," 3 ed., Oxford Univ. Press, London (1941).
2. Barnes, G. T., and V. K. La Mer, in "Retardation of Evaporation by Monolayers," V. K. La Mer, ed., p. 9, Academic Press, New York (1962).
3. Berg, J. C., and A. Acrivos, *Chem. Eng. Sci.*, **20**, 737 (1965).
4. Blank, M., and F. J. W. Roughton, *Trans. Faraday Soc.*, **56**, 1832 (1960).
5. Blank, M., in "Retardation of Evaporation by Monolayers," V. K. La Mer, ed., p. 75, Academic Press, New York (1962).
6. ———, *J. Phys. Chem.*, **65**, 1698 (1961).
7. *Ibid.*, **66**, 1911 (1962).
8. *Ibid.*, **68**, 2793 (1964).
9. Carslaw, H. S., and J. C. Jaeger, "Conduction of Heat in Solids," 2 ed., Oxford Univ. Press, London (1959).
10. Chandrasekhar, S., "Hydrodynamic and Hydromagnetic Stability," Oxford Univ. Press, London (1961).
11. Danielli, J. F., K. G. A. Pankhurst, and A. C. Riddiford, eds., "Recent Progress in Surface Science," Vol. 1, Academic Press, New York (1964).
12. Davies, J. T., and E. K. Rideal, "Interfacial Phenomena," Academic Press, New York (1961).
13. Goodridge, F., and I. D. Robb, *Ind. Eng. Chem. Fundamentals*, **4**, 49 (1965).
14. "Handbook of Chemistry and Physics," 37 ed., Chemical Rubber Publishing Co., Cleveland, Ohio (1955).
15. Harvey, E. A., and W. Smith, *Chem. Eng. Sci.*, **10**, 274 (1959).
16. Hickman, K. C. D., *Ind. Eng. Chem.*, **44**, 1892 (1952).
17. Jarvis, N. L., C. O. Timmons, and W. A. Zisman, in "Retardation of Evaporation by Monolayers," V. K. La Mer, ed., p. 41, Academic Press, New York (1962).
18. La Mer, V. K., ed., "Retardation of Evaporation by Monolayers," Academic Press, New York (1962).
19. ———, and T. W. Healy, *Science*, **148**, 36 (1965).
20. Lynn, S., J. R. Straatemeier, and H. Kramers, *Chem. Eng. Sci.*, **4**, 49 (1955).
21. Orell, A., and J. W. Westwater, *A.I.Ch.E. J.*, **8**, 350 (1962).
22. Plevan, R. E., Ph.D. thesis, Univ. Illinois, Urbana (1965).
23. Rasof, B., *J. Franklin Inst.*, **274**, 165 (1962).
24. Scriven, L. E., and R. L. Pigford, *A.I.Ch.E. J.*, **4**, 439 (1958).
25. Spangenberg, W. G., and W. R. Rowland, *Phys. Fluids*, **4**, 743 (1961).
26. Sternling, C. V., and L. E. Scriven, *A.I.Ch.E. J.*, **5**, 514 (1959).
27. Whitaker, Stephen, and R. L. Pigford, to be published.

Manuscript received July 10, 1965; revision received March 21, 1966; paper accepted March 30, 1966.